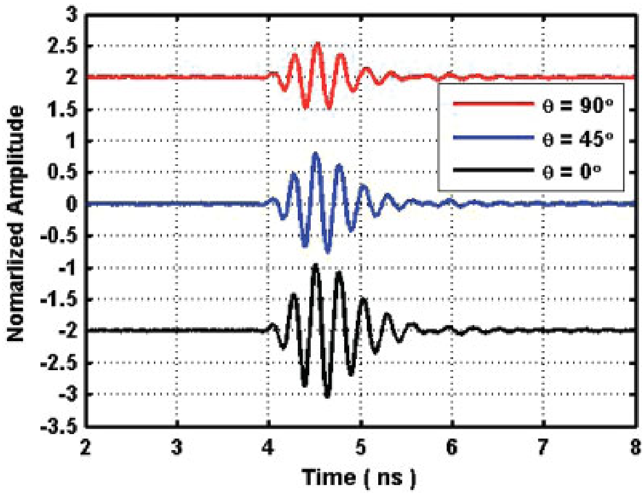

Figure 11 Radiation waveforms in the *x-z* plane of the proposed antenna. Note: Waveforms of $\theta = 0°$ and $\theta = 90°$ are shifted up and down for easy comparison. [Color figure can be viewed in the online issue, which is available at www.interscience.wiley.com]

10, the fidelity of the proposed antenna is larger than 0.85 in the whole angle range of θ, which ensures the similarity between two pulses mentioned earlier. As shown in Figure 11, for the three different observation angles of θ, the peak-to-peak normalized value is 1.05, 1.5, and 2, respectively. The value decreases to 52.5% (−5.59 dB) at $\theta = 90°$, and 75% (−2.49 dB) at $\theta = 45°$, compared with the maximum one at $\theta = 0°$.

In general, the results shown in Figures 8–11 show that the proposed antenna is very useful in TOA measurement of positioning systems with different orientation change of antenna.

5. CONCLUSION

A novel UWB square slot antenna with circular polarization is proposed and studied in this letter. It is investigated both in frequency and time domain. Results show that it has a 10-dB impedance bandwidth from 2.7 to 5.0 GHz, and a 3 dB axial ratio bandwidth from 3.5 to 4.8 GHz. This study shows that the proposed antenna can be used in lower UWB system generating circular polarization and in TOA positioning systems, and has more application value because it can be easily fabricated and integrated with other circuit components.

ACKNOWLEDGMENT

This work was supported by the ASTAR SERC under grant 052-121-0086.

REFERENCES

1. FCC Report and Order for Part 15 Acceptance of Ultra Wideband (UWB) Systems from 3.1-10.6 GHz, FCC, Washington DC, 2002.
2. C.C. Chou, K.H. Lin, and H.L. Su, Broadband circularly polarised cross-patch-loaded square slot antenna, Electronics Lett 43 (2007), 485–486.
3. J.Y. Sze, K.L. Wong, and C.C. Huang, Coplanar waveguide-fed square slot antenna for broadband circularly polarized radiation, IEEE Trans Antennas Propag 51 (2003), 2141–2144.
4. J.Y. Sze and C.C. Chang, Circularly polarized square slot antenna with a pair of inverted-L grounded strips, IEEE Antennas Wireless Propag Lett 7 (2008) 149–151.
5. Y.B. Chen, X.F. Liu, Y.C. Jiao, and F.S. Zhang, CPW-fed broadband circularly polarised square slot antenna, Electron Lett 42 (2006), 1074–1076.
6. X.M. Qing, Z.N. Chen, and H.L. Chung, Ultra-wideband circularly polarized wide-slot antenna fed by three-stub hybrid coupler, In: IEEE international conference on ultra-wideband (ICUWB), 2007, pp. 487–490; art. no. 4380994.
7. Y.X. Guo, K.W. Khoo, and L.C. Ong, Ultra-wideband circularly- polarized patch antenna, In: Asia-Pacific microwave conference, Yokohoma, Japan 2006, pp. 1644–1646.
8. T.G. Ma and S.K. Jeng, Planar miniature tapered-slot-fed annular slot antennas for ultrawide-band radios, IEEE Trans Antennas Propag 53 (2005), 1194–1202.

WIDEBAND COUPLED-FED PIFA FOR HAC PENTA-BAND CLAMSHELL MOBILE PHONE

Wei-Yu Chen and Kin-Lu Wong
Department of Electrical Engineering, National Sun Yat-Sen University, Kaohsiung 804, Taiwan; Corresponding author: chenwy@ema.ee.nsysu.edu.tw

Received 29 January 2009

ABSTRACT: *A wideband coupled-fed PIFA suitable for application in the clamshell mobile phone for achieving WWAN operation and meeting hearing-aid compatibility (HAC) standard ANSI C63.19-2007 is presented. The coupled-fed PIFA is formed by two coupled strips (a longer one and a shorter one) capacitively fed by a common feeding strip, all printed on a thin 0.8-mm FR4 substrate and folded into a small size of* $6 \times 5.8 \times 45$ *mm*^{3} *(about 1.6 cm*^{3}*). The coupled-fed PIFA is mounted at the hinge of the clamshell mobile phone and provides a very wide operating band of about 1.5 GHz (from about 0.8–2.3 GHz) to cover the penta-band operation of GSM850/900/1800/1900/UMTS. With the wideband operation obtained, the radiated E-field and H-field strengths on the* 50×50 *mm*^{2} *observation plane centered 15 mm above the center of the acoustic output of the clamshell mobile phone are evaluated to be in the M3 or M4 Category, making the mobile phone as a hearing-aid compatible communication device. The clamshell mobile phone with the coupled-fed PIFA also meets the SAR (specific absorption rate) limit of 1.6 W/kg for the 1-g head tissue.* © 2009 Wiley Periodicals, Inc.
Microwave Opt Technol Lett 51: 2369–2374, 2009; Published online in Wiley InterScience (www.interscience.wiley.com). DOI 10.1002/mop.24620

Key words: *internal mobile phone antenna; PIFA (planar inverted-F antenna); WWAN (wireless wide area network); clamshell mobile phone; hearing-aid compatibility (HAC)*

1. INTRODUCTION

The hearing-aid compatibility (HAC) standard, developed in 2001, updated in 2006 and recently revised in 2007, requires that at least half of all mobile phones on the U.S. market must have RF interference level of Category M3 or M4 of ANSI C63.19-2007 [1]. To meet the HAC standard, several studies on the near-field EM (electromagnetic) fields radiated from a mobile phone have also been reported [2–5]. Among the studies, a clamshell mobile phone embedded with a wideband coupled-fed printed loop antenna of size $5.8 \times 10 \times 45$ mm^3 (2.6 cm^3) has been shown to cover the GSM850/900/1800/1900/UMTS (824–894/890–960/1710–1880/1850–1990/1920–2170 MHz) penta-band WWAN operation and satisfy the HAC standard over the five operating bands [5]. The good HAC result makes the studied penta-band clamshell mobile phone in [5] a hearing-aid compatible communication device. However, the available promising internal antennas suitable for HAC penta-band mobile phone applications are still very few in the published articles.

In this article, we present another promising wideband internal antenna suitable for covering the GSM850/900/1800/1900/UMTS bands and satisfying the latest HAC standard ANSI C63.19-2007, effective on June 6, 2008 [1]. The proposed antenna in this study is a coupled-fed PIFA, which is different from the loop-type antenna in [5, 6] and shows a small occupied volume of 6 × 5.8 × 45 mm^3 or about 1.6 cm^3 only, much smaller than that (about 2.6 cm^3) in [6]. The coupled-fed PIFA has a simple structure and comprises two coupled strips of a longer one and a shorter one, both capacitively fed by a common feeding strip. The proposed PIFA is easy to fabricate at low cost by printing on a thin dielectric substrate and is to be mounted at the hinge of the clamshell mobile phone for WWAN operation. Although having a simple structure, the proposed PIFA can generate a wide operating band to cover the GSM850/900/1800/1900/UMTS bands. In addition, also largely owing to the wideband property obtained [5], the near-field EM fields evaluated by using the HAC simulation model provided by SPEAG SEMCAD [7] are found to meet the HAC standard ANSI C63.19-2007. That is, the clamshell mobile phone with the proposed coupled-fed PIFA can be used as an HAC communication device. Details of the proposed coupled-fed PIFA are described. The radiation characteristics including the HAC and SAR [8–12] results are also presented.

2. THE PROPOSED ANTENNA

Figure 1(a) shows the geometry of the proposed wideband coupled-fed PIFA for the HAC clamshell mobile phone. The coupled-fed PIFA occupies a volume of 6 × 5.8 × 45 mm^3 or about 1.6 cm^3 only. The photos of the fabricated antenna are shown in Figure 1(b), and its detailed dimensions of the metal pattern of the PIFA in the planar structure are given in Figure 1(c). The antenna is mounted at the hinge of the clamshell mobile phone. Compared with the general bar-type mobile phone, the clamshell mobile phone [13–21] is convenient to accommodate a larger display, which is attractive for multimedia communications and is becoming popular on the market for mobile users. The clamshell mobile phone comprises two separate ground planes of same size (45 × 75 mm^2). One is the main ground plane printed on a 0.8 mm thick FR4 substrate for the keypad, the microphone, the battery, and so forth. The FR4 substrate can also be considered as the system circuit board of the practical clamshell mobile phone. The other one is the upper ground plane fabricated using a 0.2 mm thick copper plate which can be considered as the cover of the clamshell mobile phone and usually accommodates the speaker, the embedded digital camera, the LCD display, and so forth.

The two ground planes are connected by a connecting strip of 1 mm in width and 8 mm in length. To simulate the clamshell mobile phone in the talk condition, the upper ground plane is set to have an angle α of 105° to the connecting strip; in other words, the upper ground plane has an inclination angle of 15° to the axis of the mobile phone, which is reasonable for general clamshell mobile phones in the talk condition.

As shown in Figure 1(c), the coupled-fed PIFA is printed on a 0.8 mm FR4 substrate and is formed by a longer coupled strip and a shorter coupled strip, both are capacitively fed by a common feeding strip. The longer coupled strip has a length of 61.5 mm, which is about 0.18λ at 900 MHz, and is excited by the feeding strip through a small coupling gap (gap1 = 0.4 mm). The shorter coupled strip has a length of 26.5 mm, which is about 0.19λ at 2200 MHz, and is also excited by the same feeding strip through a small coupling gap (gap2 = 0.3 mm). Note that owing to the

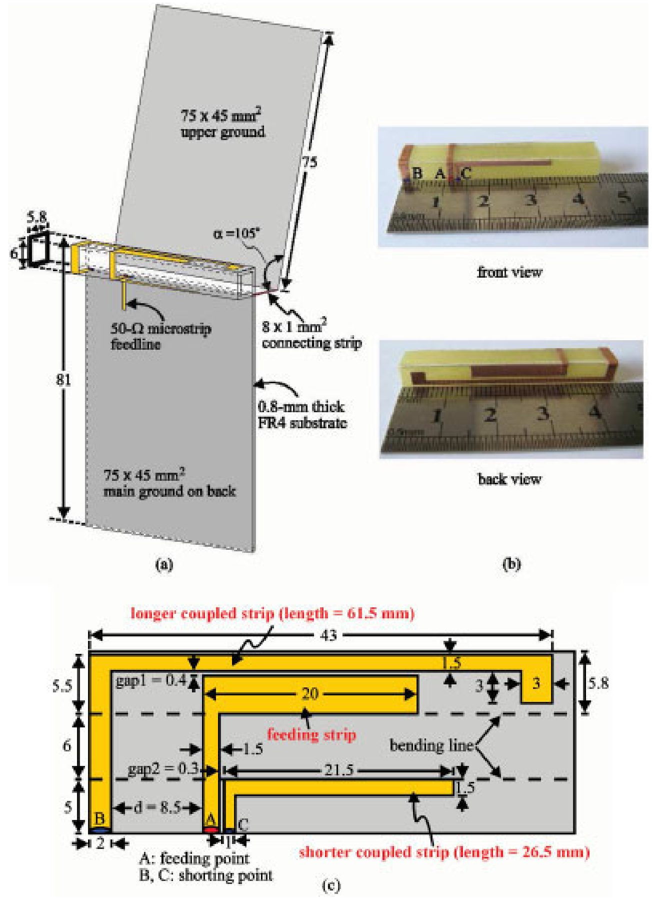

Figure 1 (a) Geometry of the proposed wideband coupled-fed PIFA for the HAC clamshell mobile phone. (b) Photos of the fabricated antenna. (c) Dimensions of the metal pattern of the antenna in the planar structure. [Color figure can be viewed in the online issue, which is available at www.interscience.wiley.com]

dielectric substrate effect which decreases the required length for quarter-wavelength resonant mode excitation, both the longer and shorter coupled strips can generate a 0.25-wavelength resonant mode at about 900 and 2200 MHz in the proposed PIFA.

Furthermore, for the feeding strip itself, it has a length of about 34 mm, corresponding to about 0.18λ at 1600 MHz. One end (point A) of the feeding strip is connected to the 50-Ω microstrip feedline printed on the front surface of the FR4 substrate or the system circuit board. The feeding strip not only successfully excites the two coupled strips, it can also work as an effective radiator (an inverted-L monopole in this study) and generate a wide 0.25-wavelength resonant mode at about 1600 MHz, which incorporates the two 0.25-wavelength resonant modes at about 900 and 2200 MHz to from a wide operating band of about 1.5 GHz (from about 0.8 to 2.3 GHz) for the proposed PIFA to cover the desired GSM850/900/1800/1900/UMTS operation. Note that the behavior of the feeding strip working as both an exciter and a radiator in the proposed coupled-fed PIFA is advantageous over the corresponding feeding strip in the internal coupled-fed mobile device antennas which mainly work as an exciter only [22–26]. This advantageous behavior of the feeding strip results in a simple structure for the proposed PIFA, yet it can still generate a wide operating band for the penta-band WWAN operation.

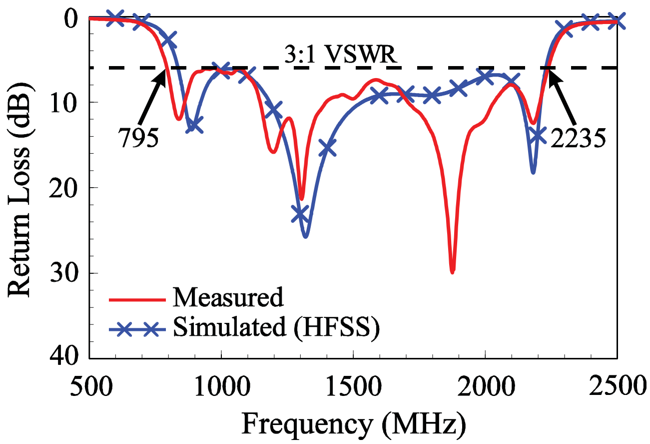

Figure 2 Measured and simulated return loss for the proposed antenna. [Color figure can be viewed in the online issue, which is available at www.interscience.wiley.com]

3. RESULTS AND DISCUSSION

The proposed antenna was fabricated and tested. Figure 2 shows the measured and simulated return loss for the fabricated prototype. The simulated results are obtained using Ansoft HFSS [27] and are seen to agree with the measured data. A wide operating band of about 1.5 GHz, ranging from 810 to 2305 MHz with the return loss better than 3:1 VSWR, is obtained. The 3:1 VSWR definition is generally adopted for the internal mobile device antenna for WWAN operation. To analyze the excitation mechanism in this design, Figure 3 shows the simulated (HFSS) return loss and input impedance for the proposed antenna and the case without the shorter coupled strip. From the return loss shown in Figure 3(a), it is clear to see that the shorter coupled strip contributes a resonant mode at about 2.2 GHz to the proposed antenna, thus resulting the coverage of the UMTS (1920∼2170 MHz) operation. This additional mode at about 2.2 GHz can also be clearly seen in Figure 3(b) (mode 3 in the figure) where the simulated input impedance is shown. Two resonant modes (mode 1 and 2) at about 900 and 1600 MHz are also seen, which are respectively contributed by the longer coupled strip and the feeding strip as discussed in Section 2. It is also observed that the input impedance of mode 2 shows a smooth variation in its real part (input resistance) and imaginary part (input reactance), which results in dual-resonance excitation (two resonances at about 1300 and 1800 MHz) as shown in Figure 3(a) for the proposed antenna.

Effects of the feeding-strip position *d* to the longer coupled strip [Fig. 1(c)] on the impedance matching of the antenna are also studied. Figure 4 shows the simulated (HFSS) return loss for the feeding-strip position *d* varied from 6.5 to 10.5 mm, with other dimensions the same as given in Figure 1. Large effects on the two resonant modes at about 900 and 2200 MHz contributed by the longer and shorter coupled strips are seen. On the other hand, relatively small effects on the dual-resonant mode centered at about 1600 MHz are observed. This is reasonable since the dual-resonant mode is mainly contributed by the feeding strip excited as a 0.25-wavelength monopole as discussed in Section 2, and, thus, the variations in the position *d* are not expected to cause large effects on the impedance matching of the excited dual-resonant mode.

Figure 5 plots the measured three-dimensional (3-D) total-power radiation patterns of the proposed antenna at 859, 925, 1795, 1920, and 2045 MHz (central frequencies of the five operating bands). Dipole-like radiation patterns and omnidirectional

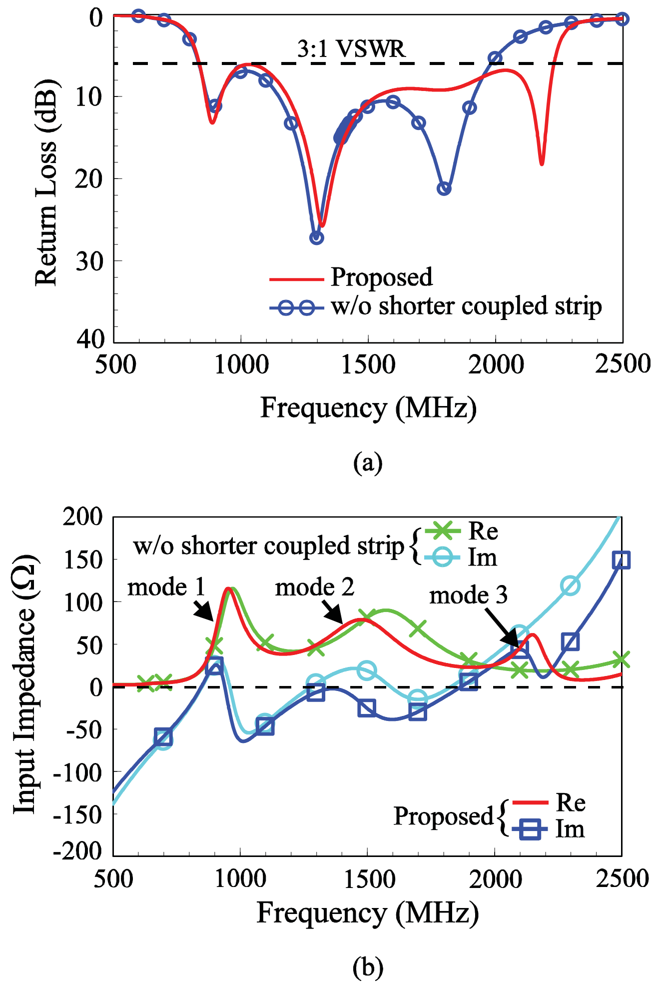

Figure 3 (a) Simulated return loss and (b) input impedance for the proposed antenna and the case without the shorter coupled strip. [Color figure can be viewed in the online issue, which is available at www.interscience.wiley.com]

radiation in the azimuthal plane are seen at 859 and 925 MHz. For higher frequencies at 1795, 1920, and 2045 MHz, more variations in the radiation patterns are observed. However, the radiation patterns are still close to omnidirectional in the azimuthal plane,

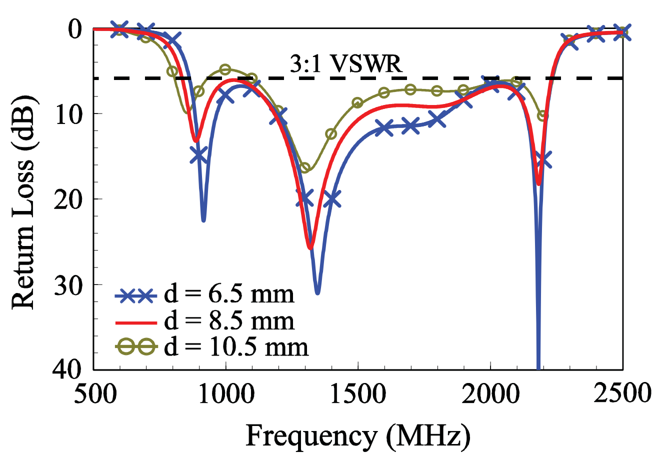

Figure 4 Simulated return loss for the proposed antenna as a function of the feeding-strip position *d*. Other dimensions are the same as given in Figure 1. [Color figure can be viewed in the online issue, which is available at www.interscience.wiley.com]

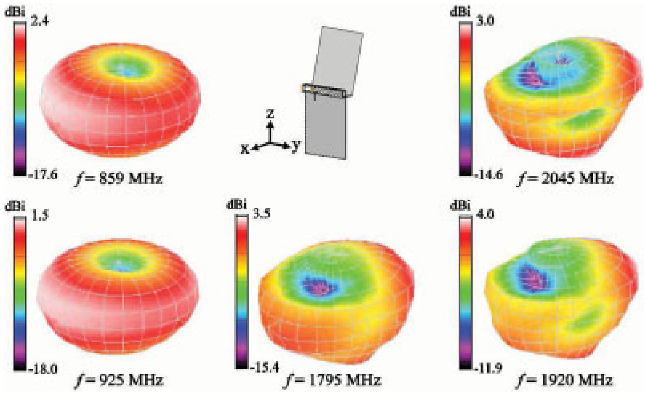

Figure 5 Measured 3-D radiation patterns of the proposed antenna. [Color figure can be viewed in the online issue, which is available at www.interscience.wiley.com]

which is attractive for practical applications. This is in part owing to the presence of the two ground planes in the clamshell mobile phone which also function as a part of the radiator.

Figure 6 shows the measured antenna gain and radiation efficiency of the proposed antenna. Over the GSM850/900 bands shown in Figure 6(a), the antenna gain is varied from about 0.7–2.6 dBi, and the radiation efficiency is in the range of 58–92%. For the GSM1800/1900/UMTS bands shown in Figure 6(b), the antenna

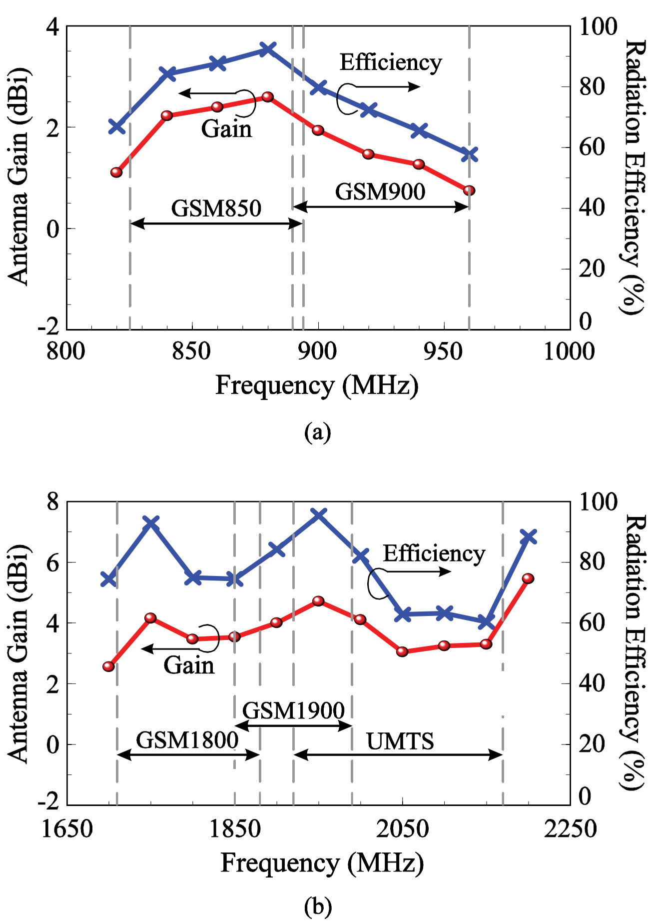

Figure 6 Measured antenna gain and radiation efficiency of the proposed antenna. (a) GSM850/900 bands. (b) GSM1800/1900/UMTS bands. [Color figure can be viewed in the online issue, which is available at www.interscience.wiley.com]

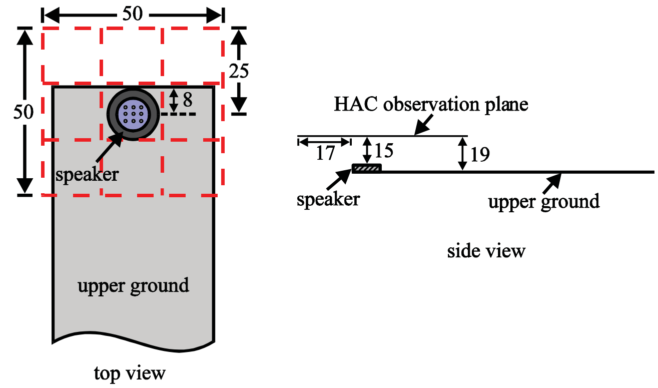

Figure 7 HAC simulation model of the studied clamshell mobile phone shown in Figures 1; the HAC observation plane is set at the top edge of the upper ground where the speaker is located. [Color figure can be viewed in the online issue, which is available at www.interscience.wiley.com]

gain is ranged from 2.8 to 4.6 dBi, while the radiation efficiency is about 60–95%. The results indicate that acceptable radiation characteristics are obtained for the propsoed antenna.

With the aid of SEMCAD simulation [7], the HAC and SAR results of the proposed antenna are also analyzed. Figure 7 shows the HAC simulation model of the studied clamshell mobile phone shown in Figure 1. The HAC observation plane of 50 × 50 mm^2 divided into 9 cells is set at the top edge of the upper ground plane where the speaker is located. Notice that the observation plane is 15 mm above the speaker (assumed to be 4 mm in thickness in the study) following the testing criterion of HAC standard ANSI C63.19-2007 and is 19 mm above the upper ground plane as shown in the figure. Also note that the latest standard ANSI C63.19-2007 relieves the testing distance of the observation plane to the speaker of the mobile phone from 10 mm in ANSI C63.19-2006 to 15 mm

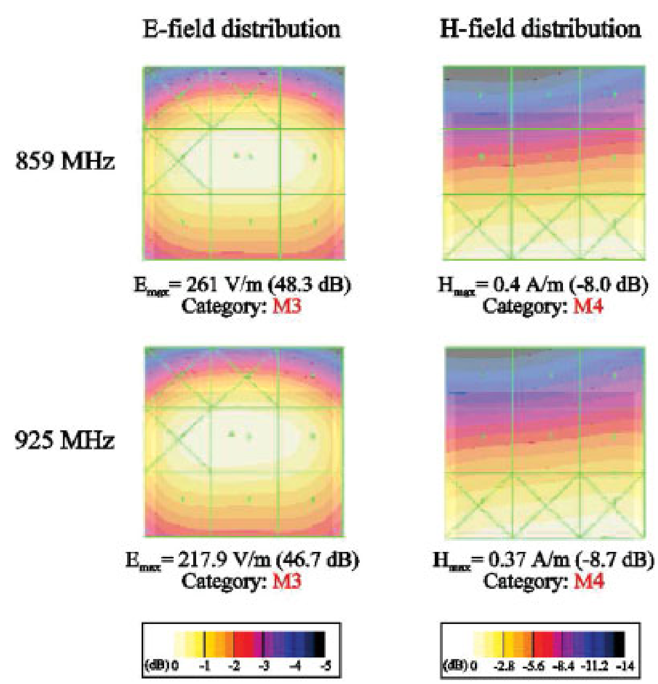

Figure 8 Simulated near-field (E-field and H-field) distributions at 859 and 925 MHz on the HAC observation plane of the simulation model shown in Figure 7. [Color figure can be viewed in the online issue, which is available at www.interscience.wiley.com]

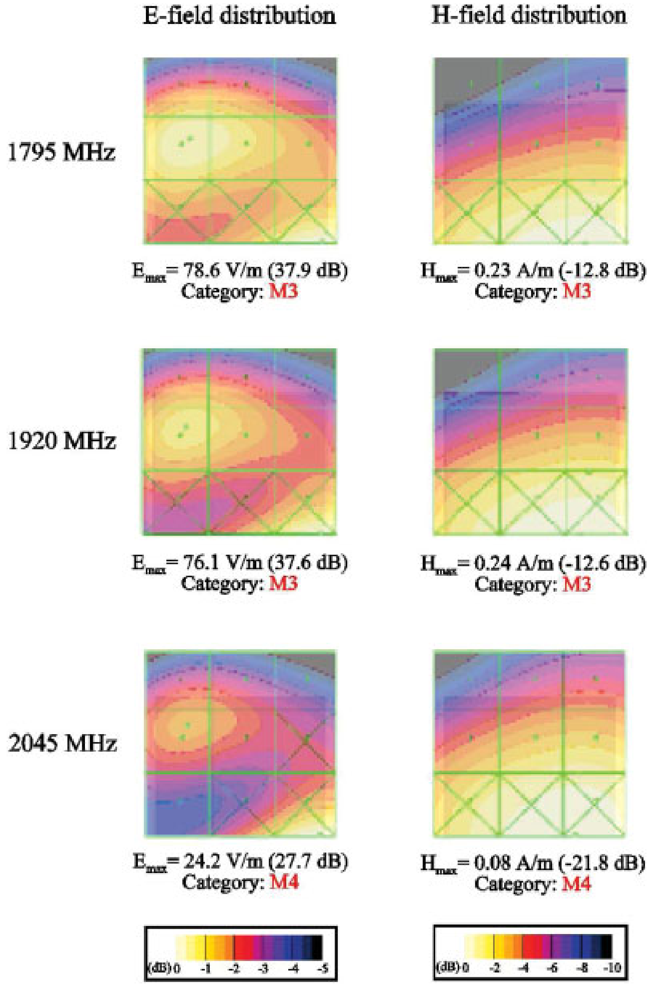

Figure 9 Simulated near-field (E-field and H-field) distributions at 1795, 1920 and 2045 MHz on the HAC observation plane of the simulation model shown in Figure 7. [Color figure can be viewed in the online issue, which is available at www.interscience.wiley.com]

as indicated in Figure 7. Figure 8 shows the simulated near-field (E-field and H-field) distributions at 859 and 925 MHz on the HAC observation plane, whereas the results at 1795, 1920, and 2045 MHz are shown in Figure 9. In the study, the testing power is 33 dBm (2 W continuous wave power) at 859 and 925 MHz, 30 dBm (1 W continuous wave power) at 1795 and 1920 MHz, and 21 dBm (0.125 W continuous wave power) at 2045 MHz. On the basis of rating methodology provided by the ANSI standard, the E-field and H-field strengths are determined by excluding three consecutive cells along the boundary of the observation plane that have the strongest field strengths [see the three crossed cells in each near-field distribution shown in the Figure]. From the results, the studied clamshell mobile phone with the proposed antenna falls into the M3 or M4 Category [4, 5] for all five operating frequencies; that is, the clamshell mobile phone studied can be considered as an HAC communication device [1] for WWAN operation over the GSM850/900/1800/1900/UMTS bands.

Figure 10 shows the SAR simulation model of the studied clamshell mobile phone shown in Figure 1. The simulation phantom head is also provided by SEMCAD [7]. The mobile phone is inclined to the vertical line shown in the figure by 60°, and the upper ground is spaced with a distance of 4 mm to the phantom ear (i.e., the speaker is attached to the phantom ear). On the basis of SAR simulation model in Figure 10, the simulated 1-g SAR

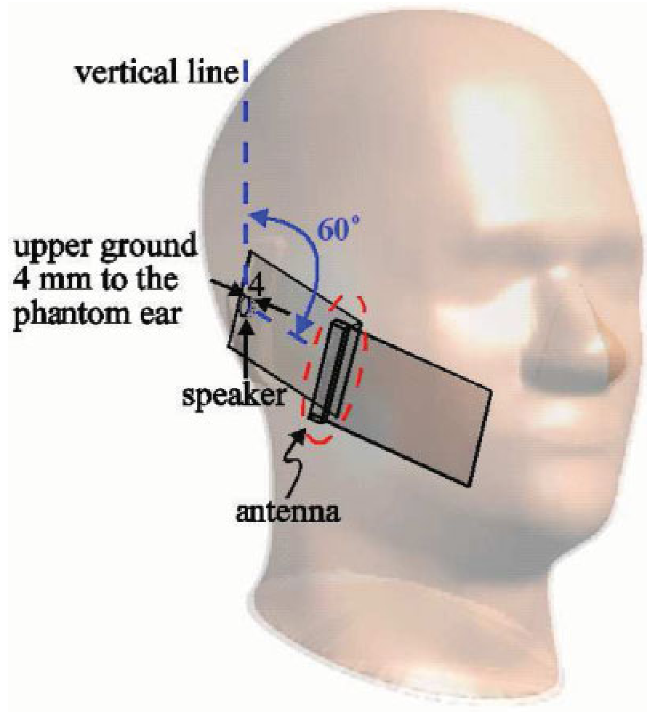

Figure 10 SAR simulation model of the studied clamshell mobile phone shown in Figure 1. [Color figure can be viewed in the online issue, which is available at www.interscience.wiley.com]

distributions at 859, 925, 1795, 1920, and 2045 MHz are shown in Figure 11. At 859 and 925 MHz, the SAR is tested using 24 dBm, whereas at 1795, 1920, and 2045 MHz, the SAR is tested using 21 dBm. Note that the testing power for SAR analysis in the GSM system (GSM850/900/1800/1900 system) is 9 dB less than that for HAC analysis, which is because a user channel in the GSM system is 1/8 of a time slot only. Also note that, as shown in the figure, the

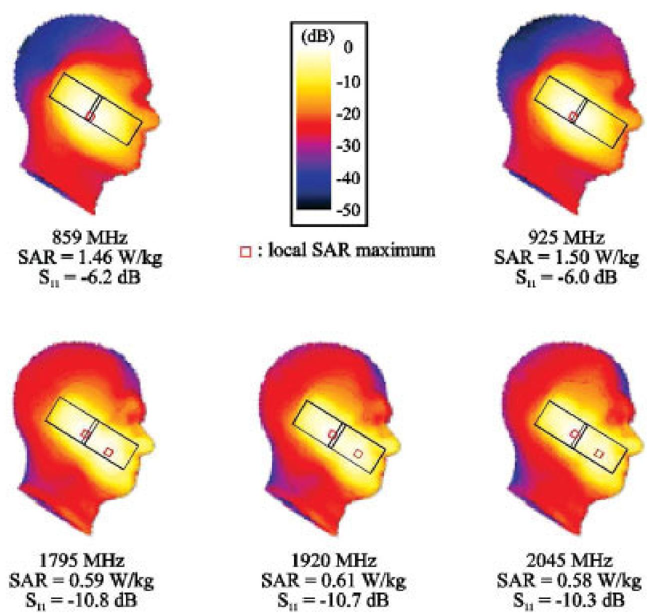

Figure 11 Simulated 1-g SAR distributions for the studied clamshell mobile phone with the proposed antenna shown in Figure 1. [Color figure can be viewed in the online issue, which is available at www.interscience.wiley.com]

reflection coefficient S_{11} of the proposed antenna is still about or better than −6.0 dB (3:1 VSWR) when the studied clamshell mobile phone is attached to the phantom head. From the SAR results obtained (1.46 W/kg at 859 MHz, 1.50 W/kg at 925 MHz, 0.59 W/kg at 1795 MHz, 0.61 W/kg at 1920 MHz, and 0.58 W/kg at 2045 MHz), it is clear to see that the proposed antenna meets the SAR specification (1.60 W/kg) for practical applications. From the SAR distributions shown in the figure, it is seen that there are two local SAR maxima at higher frequencies (1795, 1920, and 2045 MHz), whereas there is only one local SAR maximum at lower frequencies (859 and 925 MHz). This behavior explains the SAR results obtained, because the presence of two local SAR maxima suggests that the radiation energy is more uniformly distributed at higher frequencies than at lower frequencies; hence decreased SAR results will be obtained at higher frequencies.

4. CONCLUSIONS

A promising wideband coupled-fed PIFA for application as an internal clamshell mobile phone antenna has been proposed and studied. The proposed antenna occupies a small volume of $6 \times 5.8 \times 45$ mm^3 or about 1.6 cm^3 only, yet it shows a wide operating band to cover GSM850/900/1800/1900/UMTS penta-band WWAN operation. In addition, over the five operating bands, the clamshell mobile phone with the proposed antenna meets the HAC standard ANSI C63.19-2007 and the 1-g SAR limit of 1.6 W/kg. That is, the studied clamshell mobile phone in the study can be considered as an HAC communication device for WWAN operation.

REFERENCES

1. ANSI. American national standard for method of measurement of compatibility between wireless communication devices and hearing aids (ANSI C63.19-2007, revision ANSI C63.19-2006), American National Standards Institute, New York, 2007.
2. M. Okoniewski and M.A. Stuchly, Modeling of interaction of electromagnetic fields from a cellular phone with hearing aids, IEEE Trans Microwave Theory Tech 46 (1998), 1686–1693.
3. K. Caputa, N.A. Stuchly, M. Skopec, H.I. Bassen, P. Ruggera, and M. Kanda, Evaluation of electromagnetic interference from a cellular telephone with a hearing aid, IEEE Trans Microwave Theory Tech 48 (2000), 2148–2154.
4. T. Yang, W.A. Davis, W.L. Stutzman, and M.C. Huynh, Cellular-phone and hearing-aid interaction: An antenna solution, IEEE Antennas Propagat Magn 50 (2008), 51–65.
5. K.L. Wong and M.F. Tu, Hearing aid-compatible internal penta-band antenna for clamshell mobile phone, Microwave Opt Technol Lett, in press.
6. K.L. Wong and S.Y. Tu, Ultra-wideband coupled-fed loop antenna for penta-band folder-type mobile phone, Microwave Opt Technol Lett 50 (2008), 2706–2712.
7. Available at: http://www.semcad.com, SPEAG SEMCAD, Schmid and Partner Engineering AG.
8. O. Kivekas, J. Ollikainen, T. Lehtiniemi, and P. Vainikainen, Bandwidth, SAR, and efficiency of internal mobile phone antennas, IEEE Trans Electromagn Compatibility 46 (2004), 71–86.
9. Z. Li and Y. Rahmat-Samii, Optimization of PIFA-IFA combination in handset antenna design, IEEE Trans Antennas Propagat 53 (2005), 1770–1777.
10. J.C. Lin, Specific absorption rates induced in head tissues by microwave radiation from cell phones, Microwave 2 (2001), 22–25.
11. Y.W. Chi and K.L. Wong, Compact multiband folded loop chip antenna for small-size mobile phone, IEEE Trans Antennas Propagat 56 (2008), 3797–3803.
12. M.R. Hsu and K.L. Wong, Seven-band folded-loop chip antenna for WWAN/WLAN/WiMAX operation in the mobile phone, Microwave Opt Technol Lett 51 (2009), 543–549.
13. C.I. Lin and K.L. Wong, Printed monopole slot antenna for penta-band operation in the folder-type mobile phone, Microwave Opt Technol Lett 50 (2008), 2237–2241.
14. B.S. Collins, Improving the RF performance of clamshell handsets, Proc IEEE International Workshop on Antenna Technology: Small Antennas and Meta-materials (2006), 265–268.
15. K.L. Wong, Y.W. Chi, B. Chen, and S. Yang, Internal DTV antenna for folder-type mobile phone, Microwave Opt Technol Lett 48 (2006), 1015–1019.
16. K.L. Wong, W.C. Su, and F.S. Chang, Wideband internal folded planar monopole antenna for UMTS/WiMAX folder-type mobile phone, Microwave Opt Technol Lett 48 (2006), 324–327.
17. K.L. Wong, S.W. Su, C.L. Tang, and S.H. Yeh, Internal shorted patch antenna for a UMTS folder-type mobile phone, IEEE Trans Antennas Propagat 53 (2005), 3391–3394.
18. S.W. Su and K.L. Wong, Integrated internal PIFA for UMTS operation of clamshell mobile phones, Microwave Opt Technol Lett 46 (2005), 546–548.
19. P.L. Teng, C.Y. Chiu, and K.L. Wong, Internal planar monopole antenna for GSM/DCS/PCS folder-type mobile phone, Microwave Opt Technol Lett 39 (2003), 106–108.
20. P.L. Teng, T.W. Chiou, and K.L. Wong, Planar inverted-F antenna with a bent, meandered radiating arm for GSM/DCS operation, Microwave Opt Technol Lett 38 (2003), 73–75.
21. T. Sugiyama, H. Horita, Y. Shirakawa, M. Ikegaya, S. Takaba, and H. Tate, Triple-band internal antenna for clamshell type mobile phone, Hitachi Cable Review (2003), 26–31.
22. K.L. Wong and S.J. Liao, Uniplanar coupled-fed printed PIFA for WWAN operation in the laptop computer, Microwave Opt Technol Lett 51(2009), 549–554.
23. C.H. Chang, K.L. Wong, and J.S. Row, Coupled-fed small-size PIFA for penta-band folder-type mobile phone application, Microwave Opt Technol Lett 51 (2009), 18–23.
24. K.L. Wong and C.H. Huang, Printed PIFA with a coplanar coupling feed for penta-band operation in the mobile phone, Microwave Opt Technol Lett 50 (2008), 3181–3186.
25. C.H. Chang and K.L. Wong, Internal coupled-fed shorted monopole antenna for GSM850/900/1800/1900/UMTS operation in the laptop computer, IEEE Trans Antennas Propagat 56 (2008), 3600–3604.
26. K.L. Wong and C.H. Huang, Bandwidth-enhanced internal PIFA with a coupling feed for quad-band operation in the mobile phone, Microwave Opt Technol Lett 50 (2008), 683–687.
27. Available at: http://www.ansoft.com/products/hf/hfss/, Ansoft Corporation HFSS, Pittsburgh, PA.

ELECTROSTATIC CAPACITANCES FOR CARBON NANOTUBE INTERCONNECTS

V. Parkash and Ashok K. Goel
Department of Electrical and Computer Engineering, Michigan Technological University, Houghton, MI 49931; Corresponding author: goel@mtu.edu

Received 31 January 2009

ABSTRACT: *Carbon nanotubes are promising candidates for futuristic nanoelectronic applications. In this article, we present a comprehensive modeling and calculation of electrostatic capacitances for various metallic carbon nanotube systems that can be used to model interconnects in nanotechnology circuits. Capacitance results are provided for single walled, multiwalled and bundles of single-walled carbon nanotubes as functions of the various design parameters. Numerical computations were performed using the method of moments in conjunction with a*